Electromagnetic diffusion in anisotropic media

José M. Carcione[1]

Received 18 March 2010; revised 19 September 2010; accepted 4 November 2010; published 8 February 2011.

[1] I present a plane-wave analysis of anisotropic electromagnetic media at the low-frequency range, where the displacement currents can be neglected and the field is diffusive. Anisotropy is due to the conductivity tensor and the magnetic permeability is a scalar quantity. The analysis includes the energy balance (Umov-Poynting theorem) and provides expressions of measurable quantities such as the phase and energy velocities, the attenuation factor, and the skin depth as a function of frequency and propagation direction. The balance of energy allows the identification of the stored and dissipated energy densities, which are related to the magnetic energy and the conductive part of the electric energy. For a real conductivity tensor, the stored energy equals the dissipated energy. I also establish fundamental relations, e.g., the scalar product between the slowness vector and the power-flow vector is equal to the energy density. For uniform plane waves, the phase velocity is the projection of the energy velocity vector onto the propagation direction and a similar relation is obtained by replacing the energy velocity with a velocity related to the dissipated energy. I have also obtained the Green function for an azimuthally isotropic medium (transverse isotropy), which is used to calculate transient fields.

Citation: Carcione, J. M. (2011), Electromagnetic diffusion in anisotropic media, *Radio Sci.*, *46*, RS1010, doi:10.1029/2010RS004402.

1. Introduction

[2] Electromagnetic (EM) propagation at low frequencies (EM diffusion) is used in a number of applications, such as geothermal exploration [*Pellerin et al.*, 1996], evaluation of hydrocarbon resources by mapping the subseafloor resistivity [*Eidesmo et al.*, 2002], EM induction in boreholes and logging while drilling [*Wang and Signorelli*, 2004], magnetotelluric problems [*Mackie et al.*, 1993; *Yin and Maurer*, 2001], and geoelectrical surveys for groundwater and mineral exploration [*Oristaglio and Hohmann*, 1984].

[3] The theory of EM diffusion in isotropic media is well established [see, e.g., *Ward and Hohmann*, 1988]. Anisotropy has been taken into account to model magnetotelluric fields, using a propagation matrix algorithm in 1-D layered models, where the conductivity is homogeneous both laterally and vertically within each layer [*Mann*, 1965; *Loewenthal and Landisman*, 1973; *Abramovici*, 1974; *Kováčiková and Pek*, 2002]. In all these works no analysis of the physics in 3-D space is performed. At most, the wave numbers along the vertical direction are obtained. This is because they only consider the z direction and then there is no dependence with the propagation angle in their equations. In fact, the study of anisotropic diffusion in three dimensions and from the point of view of the energy balance has not given much attention in the geophysical literature. An analysis has been performed by *Carcione and Schoenberg* [2000] and *Carcione* [2007], who considered the high-frequency range (waves), where the dielectric permittivity plays an important role. Analogies can be performed with the theory of elasticity to establish mathematical and physical formulations [*Carcione and Cavallini*, 1995; *Carcione and Helbig*, 2008].

[4] There are many material configurations in the subsurface that might lead to anisotropy [*Negi and Saraf*, 1989]. The geophysical motivation behind the use of an electrically anisotropic description of the Earth are given by *Mann* [1965], *Carcione* [1996], *Weidelt* [1998], *Anderson et al.* [2001], *Carcione and Schoenberg* [2000], *Wang and Fang* [2001], and *Weiss and Newman* [2002]. It might be that there are some preferred directions in the subsurface rocks, or some preferred orientation of grains in the sediments. Compaction, fine layering or a pronounced strike direction might lead to effective anisotropy.

[1]Istituto Nazionale di Oceanografia e di Geofisica Sperimentale, Trieste, Italy.

Copyright 2011 by the American Geophysical Union.
0048-6604/11/2010RS004402

Alternations of sandstone and shales may give reservoir anisotropy [*Carcione and Seriani*, 2000; *Davydycheva et al.*, 2003].

[5] The paper is organized as follows. First, Maxwell's equations are given, in the inhomogeneous and homogeneous cases. Then, I perform a plane-wave analysis and obtain the Kelvin-Christoffel eigensystem, whose eigenvalues yield the phase velocities and skin depth as a function of the conductivity components, frequency and propagation direction. The energy balance (Umov-Poynting theorem) is then established to obtain expressions of the energy densities and energy velocity. Finally, I obtain the Green function for a uniaxial medium.

2. Maxwell's Equations for General Anisotropic Media

[6] In vector notation, Maxwell's equations, neglecting the displacement currents, are [e.g., *Carcione*, 2007]

$$\begin{aligned} \nabla \times \mathbf{E} &= -\partial_t \mathbf{B} + \mathbf{M}, \\ \nabla \times \mathbf{H} &= \mathbf{J}_I + \mathbf{J}_S \equiv \mathbf{J}, \end{aligned} \tag{1}$$

where the vectors $\mathbf{E}$, $\mathbf{H}$, $\mathbf{B}$, $\mathbf{J}_I$, $\mathbf{J}_S$, and $\mathbf{M}$ are the electric field intensity, the magnetic field intensity, the magnetic flux density, the induced current density, the electric source current, and the magnetic source density, respectively. In general, they depend on the Cartesian coordinates $(x_1, x_2, x_3) = (x, y, z)$, and the time variable t. I have used the compact notation $\partial_t \equiv \partial/\partial_t$.

[7] Additional constitutive equations are needed. These are $\mathbf{J}_I = \boldsymbol{\sigma} \cdot \mathbf{E}$ and $\mathbf{B} = \mu\mathbf{H}$, where $\boldsymbol{\sigma}$, the conductivity tensor, is a real, symmetric and positive definite tensor, and μ, the magnetic permeability, is a scalar quantity, and the dot denotes ordinary matrix multiplication. Substituting the constitutive equations into equations (1) gives

$$\begin{aligned} \nabla \times \mathbf{E} &= -\mu\partial_t \mathbf{H} + \mathbf{M}, \\ \nabla \times \mathbf{H} &= \boldsymbol{\sigma} \cdot \mathbf{E} + \mathbf{J}_S, \end{aligned} \tag{2}$$

which are a system of six scalar equations in six scalar unknowns.

[8] In this work, I am concerned with triclinic media, where at each point of the space the conductivity tensor is nondiagonal. However, the tensor can always be rotated to obtain its expression in its principal coordinate system

$$\boldsymbol{\sigma} = \begin{pmatrix} \sigma_1 & 0 & 0 \\ 0 & \sigma_2 & 0 \\ 0 & 0 & \sigma_3 \end{pmatrix}. \tag{3}$$

Although the magnetic permeability is commonly assumed to be that of free space, some soils have a significantly higher value [*Olhoeft and Capron*, 1994], hence, μ can vary arbitrarily in space. In some cases, such as the CSEM problems μ is assumed to be spatially constant [*Eidesmo et al.*, 2002].

[9] From equation (1) I obtain a vector equation for the electric field

$$-\partial_t \mathbf{E} = \boldsymbol{\sigma}^{-1} \cdot \left[\nabla \times \left(\mu^{-1}\nabla \times \mathbf{E}\right) + \partial_t \mathbf{J}_S + \nabla \times \mathbf{M}\right]. \tag{4}$$

Note that

$$\nabla \times (\mu^{-1}\nabla \times) = \begin{pmatrix} -(\partial_2\mu^{-1}\partial_2 + \partial_3\mu^{-1}\partial_3) & \partial_2\mu^{-1}\partial_1 & \partial_3\mu^{-1}\partial_1 \\ \partial_1\mu^{-1}\partial_2 & -(\partial_1\mu^{-1}\partial_1 + \partial_3\mu^{-1}\partial_3) & \partial_3\mu^{-1}\partial_2 \\ \partial_1\mu^{-1}\partial_3 & \partial_2\mu^{-1}\partial_3 & -(\partial_1\mu^{-1}\partial_1 + \partial_2\mu^{-1}\partial_2) \end{pmatrix}, \tag{5}$$

where I have denoted $\partial/\partial x_i$ by ∂_i for brevity.

[10] Following *Badea et al.* [2001] and *Stalnaker* [2004], I consider the case

$$\nabla \cdot \mathbf{J} = \nabla \cdot (\boldsymbol{\sigma} \cdot \mathbf{E}) = 0, \tag{6}$$

which is valid for $\nabla \cdot \mathbf{J}_S = 0$, according to equation (1), i.e., if the source current density is divergence free [*Ward and Hohmann*, 1988, equation 1.7]. This condition is satisfied by inductively coupled magnetic dipole controlled sources of the form

$$\mathbf{J}_S = \nabla \times \mathbf{A}, \tag{7}$$

where $\mathbf{A}$ is a vector. In 2-D (x, z) space, an example is $\mathbf{J}_s = (\partial_3 F, -\partial_1 F)^\top h$, where $F(\mathbf{x})$ is the spatial distribution and $h(t)$ is the time history.

[11] In homogeneous media with a diagonal conductivity tensor, equation (4) becomes

$$-\partial_t \mathbf{E} = \boldsymbol{\gamma} \cdot \nabla \times \nabla \times \mathbf{E}, \tag{8}$$

where $\boldsymbol{\gamma} = (\mu\boldsymbol{\sigma})^{-1}$. The explicit form of equation (8) is

$$\begin{aligned} -\partial_t E_1 &= \gamma_1\left[-\left(\partial_2^2 E_1 + \partial_3^2 E_1\right) + \partial_2\partial_1 E_2 + \partial_3\partial_1 E_3\right], \\ -\partial_t E_2 &= \gamma_2\left[-\left(\partial_1^2 E_2 + \partial_3^2 E_2\right) + \partial_2\partial_1 E_1 + \partial_3\partial_2 E_3\right], \\ -\partial_t E_3 &= \gamma_3\left[-\left(\partial_1^2 E_3 + \partial_2^2 E_3\right) + \partial_1\partial_3 E_1 + \partial_2\partial_3 E_2\right]. \end{aligned} \tag{9}$$

[12] Consider the 2D anisotropic case, ignoring the y dimension. The corresponding equations are

$$\begin{aligned} -\partial_t E_1 &= \gamma_1\left(-\partial_3^2 E_1 + \partial_3\partial_1 E_3\right), \\ -\partial_t E_3 &= \gamma_3\left(-\partial_1^2 E_3 + \partial_1\partial_3 E_1\right). \end{aligned} \tag{10}$$

From (6) one has $\sigma_1\partial_1 E_1 + \sigma_3\partial_3 E_3 = 0$. Combining this equation with (10) yields

$$\begin{aligned} \partial_t E_1 &= \gamma_1\partial_3^2 E_1 + \gamma_3\partial_1^2 E_1 = \Delta_\gamma E_1, \\ \partial_t E_3 &= \gamma_3\partial_1^2 E_3 + \gamma_1\partial_3^2 E_3 = \Delta_\gamma E_3, \end{aligned} \tag{11}$$

where

$$\Delta_\gamma = \gamma_1\partial_3^2 + \gamma_3\partial_1^2 = \frac{1}{\mu\sigma_3}\partial_1^2 + \frac{1}{\mu\sigma_1}\partial_3^2 \tag{12}$$

is a modified Laplacian. Note that the field components have decoupled.

[13] In 3D space, the E_3 component can be decoupled if one considers a transversely isotropic medium with $\sigma_1 = \sigma_2$. In this case, a similar procedure leads to

$$\partial_t E_3 = \Delta_\gamma E_3, \tag{13}$$

where

$$\Delta_\gamma = \gamma_1\partial_3^2 + \gamma_3\left(\partial_1^2 + \partial_2^2\right) \tag{14}$$

and a corresponding analytical solution is given below.

3. Plane-Wave Theory

[14] I assume *nonuniform* harmonic plane waves with a phase factor

$$\exp[\imath\omega(t - \boldsymbol{\xi}\cdot\mathbf{x})], \tag{15}$$

where $\boldsymbol{\xi}$, the complex slowness vector, is equivalent to $\mathbf{k}/\omega$, with $\mathbf{k}$ and ω being the wave number vector and frequency, respectively. The dot denotes the scalar product and $\imath = \sqrt{-1}$. Note the following correspondences between time and frequency domain:

$$\nabla\times \rightarrow -\imath\omega\boldsymbol{\xi}\times \quad \text{and} \quad \partial/\partial t \rightarrow \imath\omega, \tag{16}$$

where $\times$ denotes the vector product.

[15] Substituting the plane wave (15) into Maxwell's equations (2) in the absence of sources, and using (16) gives

$$\boldsymbol{\xi}\times\mathbf{E} = \mu\mathbf{H} \tag{17}$$

and

$$\boldsymbol{\xi}\times\mathbf{H} = \frac{\imath}{\omega}\boldsymbol{\sigma}\cdot\mathbf{E}. \tag{18}$$

For convenience, the medium properties are denoted by the same symbols, in both the time and frequency domains.

[16] Taking the vector product of equation (17) with $\boldsymbol{\xi}$, gives

$$\boldsymbol{\xi}\times\left(\mu^{-1}\boldsymbol{\xi}\times\mathbf{E}\right) = \boldsymbol{\xi}\times\mathbf{H}, \tag{19}$$

which, with equation (18), becomes

$$\omega\boldsymbol{\xi}\times\left(\mu^{-1}\boldsymbol{\xi}\times\mathbf{E}\right) - \imath\boldsymbol{\sigma}\cdot\mathbf{E} = 0 \tag{20}$$

for three equations for the components of $\mathbf{E}$. Alternatively, the vector product of equation (18) with $\boldsymbol{\xi}$ and use of (17) yields

$$\imath\omega\boldsymbol{\xi}\times\left(\boldsymbol{\sigma}^{-1}\cdot\boldsymbol{\xi}\times\mathbf{H}\right) + \mu\mathbf{H} = 0, \tag{21}$$

for three equations for the components of $\mathbf{H}$.

[17] The equivalent of the 3 × 3 viscoelastic Kelvin-Christoffel equations, for the electric field vector components, are

$$\left(\omega e_{ijk}\xi_j e_{kpq}\xi_p - \imath\mu\sigma_{iq}\right)E_q = 0, \tag{22}$$

where the subindices take the values 1, 2 and 3, and e_{ijk} are the elements of the Levi-Civita tensor.

[18] Similarly, the equations for the magnetic field vector components are

$$\left(\imath\omega e_{ijk}\xi_j\sigma_{kl}^{-1}e_{lpq}\xi_p + \delta_{iq}\mu\right)H_q = 0. \tag{23}$$

Rotating the conductivity tensor to the principal system of coordinates, equation (3) is obtained. There is no loss of generality in this operation. Then, the equivalent of the viscoelastic Kelvin-Christoffel equation for the electric field vector is

$$\boldsymbol{\Gamma}\cdot\mathbf{E} = \mathbf{0}, \tag{24}$$

where the EM Kelvin-Christoffel matrix is

$$\mathbf{\Gamma} = \begin{pmatrix} \imath\mu\sigma_1 + \omega\left(\xi_2^2 + \xi_3^2\right) & -\omega\xi_1\xi_2 & -\omega\xi_1\xi_3 \\ -\omega\xi_1\xi_2 & \imath\mu\sigma_2 + \omega\left(\xi_1^2 + \xi_3^2\right) & -\omega\xi_2\xi_3 \\ -\omega\xi_1\xi_3 & -\omega\xi_2\xi_3 & \imath\mu\sigma_3 + \omega\left(\xi_1^2 + \xi_2^2\right) \end{pmatrix}. \tag{25}$$

After defining

$$\eta_i = \mu\sigma_i, \quad \zeta_i = \eta_j + \eta_k, \quad j \neq k \neq i, \tag{26}$$

the dispersion relation (i.e., the vanishing of the determinant of the Kelvin-Christoffel matrix) becomes

$$\omega^2\left(\eta_1\xi_1^2 + \eta_2\xi_2^2 + \eta_3\xi_3^2\right)\xi^2 + \imath\omega\left(\eta_1\zeta_1\xi_1^2 + \eta_2\zeta_2\xi_2^2 + \eta_3\zeta_3\xi_3^2\right) - \eta_1\eta_2\eta_3 = 0. \tag{27}$$

There are only quartic and quadratic terms of the slowness components in the dispersion relation.

3.1. Slowness, Kinematic Velocities, Attenuation, and Skin Depth

[19] The slowness vector can be split into real and imaginary vectors such that $\omega\mathrm{Re}(t - \boldsymbol{\xi}\cdot\mathbf{x})$ is the phase and $\omega\mathrm{Im}(\boldsymbol{\xi}\cdot\mathbf{x})$ is the attenuation. Assume that propagation and attenuation directions coincide to produce a *uniform* plane wave, which is equivalent to a homogeneous plane wave in viscoelasticity. The slowness vector can be expressed as

$$\boldsymbol{\xi} = \xi(l_1, l_2, l_3)^\top \equiv \xi\hat{\boldsymbol{\xi}}, \tag{28}$$

where ξ is the complex slowness and $\hat{\boldsymbol{\xi}} = (l_1, l_2, l_3)^\top$ is a real unit vector, with l_i the direction cosines ($\sum_i l_i^2 = 1$). I obtain the real wave number vector and the real attenuation vector as

$$\mathrm{Re}(\boldsymbol{\xi}) \quad \text{and} \quad \boldsymbol{\alpha} = -\omega\mathrm{Im}(\boldsymbol{\xi}), \tag{29}$$

respectively.

[20] Substituting equation (28) into the dispersion relation (27) yields

$$\omega^2\left(\eta_1 l_1^2 + \eta_2 l_2^2 + \eta_3 l_3^2\right)\xi^4 + \imath\omega\left(\eta_1\zeta_1 l_1^2 + \eta_2\zeta_2 l_2^2 + \eta_3\zeta_3 l_3^2\right)\xi^2 - \eta_1\eta_2\eta_3 = 0. \tag{30}$$

It can be shown that the roots have the form

$$\xi = (1 - \imath)s, \tag{31}$$

where s is a real slowness. Note the property

$$|\xi|^2 = \imath\xi^2 = 2s^2. \tag{32}$$

[21] In terms of the complex velocity

$$v = \frac{1}{\xi}, \tag{33}$$

the phase velocity and attenuation are

$$v_p = \left[\mathrm{Re}\left(v^{-1}\right)\right]^{-1} = \frac{1}{s} \quad \text{and} \quad \alpha = -\omega\mathrm{Im}\left(v^{-1}\right) = \omega s, \tag{34}$$

respectively.

[22] The skin depth is the distance $\mathbf{d}$ for which $\exp(-\boldsymbol{\alpha}\cdot\mathbf{d}) = 1/\mathrm{e}$, where e is Napier's number, i.e., the effective distance of penetration of the signal, where $\boldsymbol{\alpha} = \alpha\hat{\boldsymbol{\xi}}$. Using equation (29) yields

$$\sum_{i=1}^{3} d_i l_i = d = \frac{1}{\alpha}, \tag{35}$$

since $d_i = d l_i$.

[23] Assume, for instance, propagation in the (1, 2) plane. Then, $l_3 = 0$ and the dispersion relation (30) is factorizable, giving

$$\left[\omega\xi^2\left(\sigma_1 l_1^2 + \sigma_2 l_2^2\right) + \imath\mu\sigma_1\sigma_2\right]\left(\omega\xi^2 + \imath\mu\sigma_3\right) = 0. \tag{36}$$

These factors give the TM and TE modes with complex velocities

$$v^{\mathrm{TM}} = (1 - \imath)\sqrt{\frac{\omega}{2\mu}\left(\frac{l_1^2}{\sigma_2} + \frac{l_2^2}{\sigma_1}\right)}, \qquad v^{\mathrm{TE}} = (1 - \imath)\sqrt{\frac{\omega}{2\mu\sigma_3}}. \tag{37}$$

In the TM (TE) case the magnetic (electric) field vector is perpendicular to the propagation plane. For obtaining the

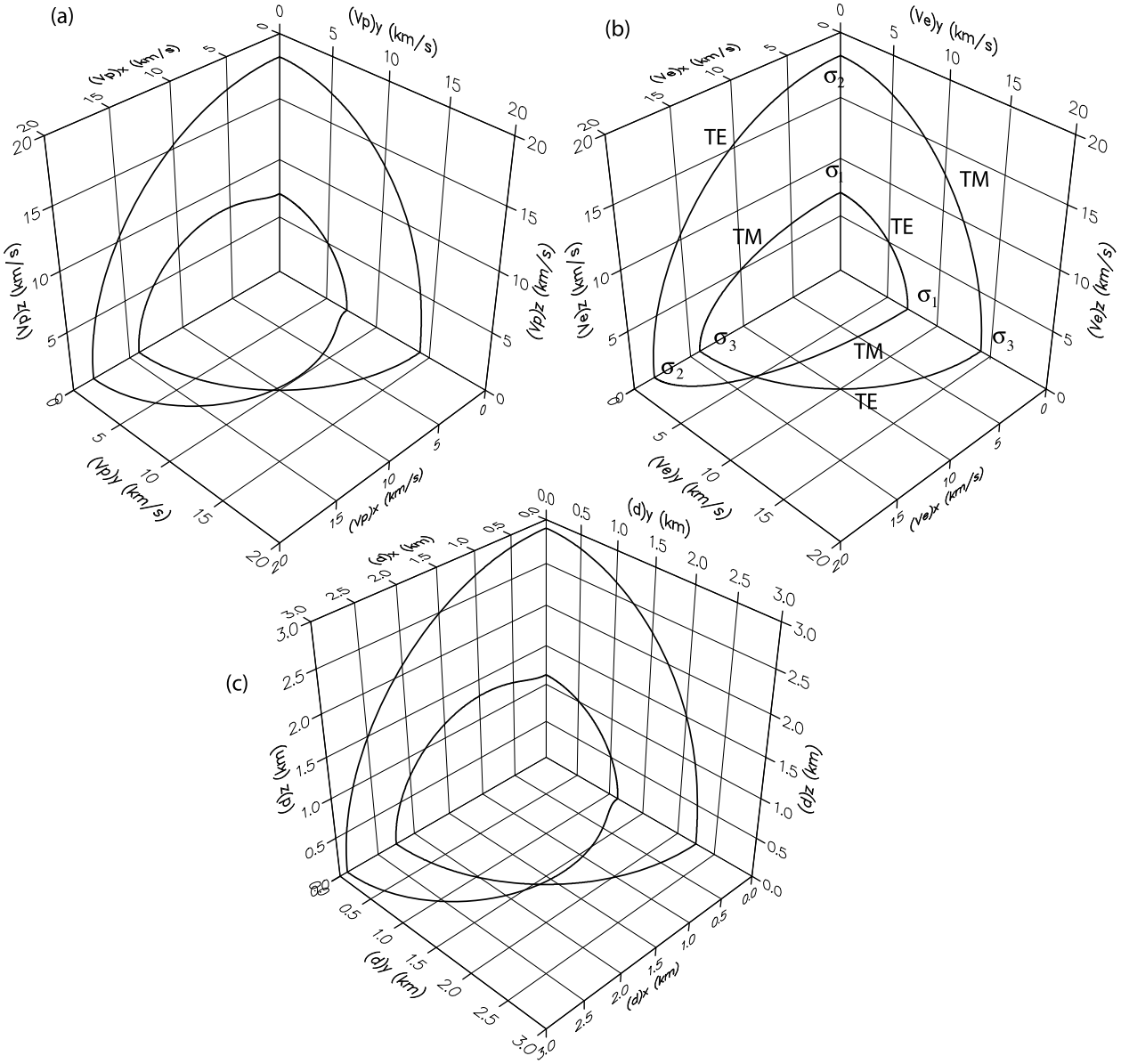

Figure 1. (a) Phase velocity, (b) energy velocity, and (c) skin depth at the Cartesian planes. The frequency is $f = 1$ Hz. The modes are indicated in Figure 1b, together with the conductivity components associated with the TE mode; $v_e^{\mathrm{TE}} = v_p^{\mathrm{TE}} \propto 1/\sqrt{\sigma_i}$ (see equations (39) and (58)).

slowness and complex velocities for the other planes, simply make the following subindex substitutions:

$$\begin{aligned} &\text{from the } (1,2)\text{plane to the } (1,3)\text{plane } (1,2,3) \rightarrow (3,1,2),\\ &\text{from the } (1,2)\text{plane to the } (2,3)\text{plane } (1,2,3) \rightarrow (2,3,1). \end{aligned} \tag{38}$$

The analysis of all three planes of symmetry gives the curves represented in Figure 1b. There exists a single conical point given by the intersection of the TE and TM modes, as can be seen in the (1,2) plane of symmetry. The location of the conical point depends on the values of the material properties. The slowness curves of the TE

modes intersecting the three orthogonal planes are circles (isotropy).

[24] Consider the TE mode. Then, the phase velocity is

$$v_p^{\mathrm{TE}} = 2\sqrt{\frac{\pi f}{\mu\sigma_3}}, \tag{39}$$

where $f = \omega/(2\pi)$ is the frequency. On the other hand, the skin depth and attenuation factor are given by

$$d^{\mathrm{TE}} = \frac{1}{\alpha^{\mathrm{TE}}} = \sqrt{\frac{1}{\pi f \mu \sigma_3}}. \tag{40}$$

The velocity increases and the skin depth decreases with frequency. In the anisotropic case, these quantities depend on the propagation angle.

3.2. Umov-Poynting's Theorem and Energy Velocity

[25] The scalar product of the complex conjugate of equation (18) with $\mathbf{E}$, use of the relation $2\imath\mathrm{Im}(\boldsymbol{\xi}) \cdot (\mathbf{E} \times \mathbf{H}^*) = (\boldsymbol{\xi} \times \mathbf{E}) \cdot \mathbf{H}^* + \mathbf{E} \cdot (\boldsymbol{\xi} \times \mathbf{H})^*$ and substitution of equation (17), gives Umov-Poynting's theorem for plane waves

$$\mathrm{Im}(\boldsymbol{\xi}) \cdot \mathbf{P} = -(\imath u_m + u_e), \tag{41}$$

where

$$\mathbf{P} = \frac{1}{2}\mathbf{E} \times \mathbf{H}^* \tag{42}$$

is the complex Umov-Poynting vector, and

$$u_e = \frac{1}{4}\mathbf{E} \cdot \frac{\boldsymbol{\sigma}^*}{\omega} \cdot \mathbf{E}^* \quad \text{and} \quad u_m = \frac{1}{4}\mu|\mathbf{H}|^2 \tag{43}$$

are the electric (dissipated) and magnetic (stored) energy densities, respectively. The superscript "*" denotes complex conjugate. The imaginary part of equation (41) gives the balance of stored energy and the real part gives the balance of dissipated energy. This equation hold for a complex conductivity tensor, i.e., including induced polarization effects [*Zhdanov*, 2008]. In this work, $\boldsymbol{\sigma}$ is real and u_m and u_e are therefore real quantities. Because of this fact, there is no electric stored energy in the diffusion process. Furthermore, it is shown in the appendix that

$$u_e = u_m \equiv u. \tag{44}$$

Therefore, the energy balance (41) is

$$\mathrm{Im}(\boldsymbol{\xi}) \cdot \mathbf{P} = -(1 + \imath)u. \tag{45}$$

The energy velocity vector, $\mathbf{v}_e$, is given by the energy power flow Re(**P**) divided by the total stored energy density, u_m. Thus,

$$\mathbf{v}_e = \frac{\mathrm{Re}(\mathbf{P})}{u}. \tag{46}$$

3.3. Fundamental Relations

[26] The scalar product of equation (17) with $\mathbf{H}^*$ and the scalar product of the complex conjugate of equation (18) with $\mathbf{E}$ yield

$$\begin{aligned} &\mathbf{H}^* \cdot (\boldsymbol{\xi} \times \mathbf{E}) = \mu\mathbf{H} \cdot \mathbf{H}^* = 4u_m, \\ &\mathbf{E} \cdot (\boldsymbol{\xi} \times \mathbf{H})^* = \mathbf{E} \cdot \left(\frac{\imath}{\omega}\boldsymbol{\sigma} \cdot \mathbf{E}\right)^* = -4\imath u_e. \end{aligned} \tag{47}$$

Using the property $\mathbf{A} \cdot \mathbf{B} \times \mathbf{C} = \mathbf{C} \times \mathbf{A} \cdot \mathbf{B}$, we obtain

$$\begin{aligned} &\mathbf{P} \cdot \boldsymbol{\xi} = 2u_m, \\ &\mathbf{P} \cdot \boldsymbol{\xi}^* = 2\imath u_e. \end{aligned} \tag{48}$$

Adding these two equations gives

$$\mathrm{Re}(\boldsymbol{\xi}) \cdot \mathbf{P} = \imath u_e + u_m. \tag{49}$$

For a real conductivity tensor, the real and imaginary parts of this equation yields

$$\begin{aligned} &\mathrm{Re}(\boldsymbol{\xi}) \cdot \mathrm{Re}(\mathbf{P}) = u, \\ &\mathrm{Re}(\boldsymbol{\xi}) \cdot \mathrm{Im}(\mathbf{P}) = u. \end{aligned} \tag{50}$$

For homogeneous waves, it is

$$\begin{aligned} &\hat{\boldsymbol{\xi}} \cdot \mathbf{v}_e = v_p, \\ &\hat{\boldsymbol{\xi}} \cdot \mathbf{v}_d = v_p, \end{aligned} \tag{51}$$

where I have used equations (33), (34), and (46), and

$$\mathbf{v}_d = \frac{\mathrm{Im}(\mathbf{P})}{u} \tag{52}$$

is a velocity associated with the dissipated energy. Similar relations are obtained in viscoelasticity and poroviscoelasticity [e.g., *Carcione*, 2007]. The first equation (51) indicates that the slowness and energy velocity surfaces are reciprocal.

3.4. The TE and TM Modes

[27] As an example, I consider the TE mode propagating in the (1,2) plane. Then,

$$\mathbf{E} = E_0(0, 0, 1)^\top \exp[\imath(\boldsymbol{\xi} \cdot \mathbf{x})], \tag{53}$$

where E_0 is a complex amplitude. By equation (17),

$$\mathbf{H} = \mu^{-1}\boldsymbol{\xi} \times \mathbf{E} = E_0\mu^{-1}\xi(l_2, -l_1, 0)^\top \exp[\imath(\boldsymbol{\xi}\cdot\mathbf{x})], \tag{54}$$

where I have assumed uniform plane waves. Substituting the electric and magnetic fields into the energy density (43) (see equation (44)) yields

$$u^{\mathrm{TE}} = \frac{1}{4\mu}|E_0|^2|v^{\mathrm{TE}}|^{-2}\exp(-2\boldsymbol{\alpha}\cdot\mathbf{x}), \tag{55}$$

where v^{TE} is given in (37), and the attenuation $\boldsymbol{\alpha}$ is given by equation (34). Alternatively,

$$u^{\mathrm{TE}} = \frac{1}{2\mu {v_p}^2}|E_0|^2\exp(-2\boldsymbol{\alpha}\cdot\mathbf{x}), \tag{56}$$

where v_p is the phase velocity (39). The TE power flow vector is

$$\mathrm{Re}(\mathbf{P}) = \frac{1}{2\mu v_p}|E_0|^2\hat{\boldsymbol{\xi}}\exp(-2\boldsymbol{\alpha}\cdot\mathbf{x}), \tag{57}$$

where $\hat{\boldsymbol{\xi}} = \hat{\mathbf{e}}_1 l_1 + \hat{\mathbf{e}}_2 l_2$ defines the wave number vector direction. From equations (46), (56), and (57) I obtain the energy velocity for TE waves propagating in the (1,2) plane as

$$\mathbf{v}_e^{\mathrm{TE}} = v_p\,\hat{\boldsymbol{\xi}}. \tag{58}$$

As in the viscoelastic case, the energy velocity equals the phase velocity when there is isotropy [e.g., *Carcione*, 2007].

[28] Performing similar calculations, the energy density and energy velocity for TM waves propagating in the (1,2) plane are

$$u^{\mathrm{TM}} = \frac{1}{4}\mu|H_0|^2\exp(-2\boldsymbol{\alpha}\cdot\mathbf{x}) \tag{59}$$

and

$$\mathbf{v}_e^{\mathrm{TM}} = -\frac{2\omega}{\mu}\mathrm{Im}\left(\frac{1}{v^{\mathrm{TM}}}\right)\left(\frac{l_1}{\sigma_2}\hat{\mathbf{e}}_1 + \frac{l_2}{\sigma_1}\hat{\mathbf{e}}_2\right), \tag{60}$$

respectively, where v^{TM} is given in (37). The expressions corresponding to the (1,3) and (2,3) planes can be obtained by making the substitutions (38).

4. Transient Analytical Solution

[29] A transient solution can be obtained to describe the amplitude of the diffusion field and test simulation codes. Consider equations (13), denoting E_3 by E. Redefining the source term, I have

$$\Delta_\gamma E - \partial_t E = J_S,$$
$$\Delta_\gamma = \gamma_1\partial_3^2 + \gamma_3\left(\partial_1^2 + \partial_2^2\right) = \frac{1}{\mu\sigma_3}\left(\partial_1^2 + \partial_2^2\right) + \frac{1}{\mu\sigma_1}\partial_3^2. \tag{61}$$

Defining $x' = x/\sqrt{\gamma_3}$, $y' = y/\sqrt{\gamma_3}$ and $z' = z/\sqrt{\gamma_1}$, I obtain

$$\Delta' E - \partial_t E = J_S, \qquad \Delta' = \frac{\partial^2}{\partial x'^2} + \frac{\partial^2}{\partial y'^2} + \frac{\partial^2}{\partial z'^2}. \tag{62}$$

The solution for the Green function is obtained for $J_S = -\delta(x', y', z')\delta(t)$. I get [*Carslaw and Jaeger*, 1984]

$$g(x, y, z, t) = \frac{1}{4\pi t}\exp\left[-r'^2/(4t)\right], \tag{63}$$

where

$$r' = \sqrt{x'^2 + y'^2 + z'^2} = \sqrt{\frac{x^2 + y^2}{\gamma_1} + \frac{z^2}{\gamma_3}}$$
$$= \sqrt{\mu}\sqrt{\sigma_3(x^2 + y^2) + \sigma_1 z^2}. \tag{64}$$

If $J_S = -\delta(x, y, z)h(t)$, the solution is given by

$$E = g * h, \tag{65}$$

where "*" denotes time convolution here.

[30] The solution corresponds to transverse isotropy, for which there are two eigen directions, and only two, for which all three tensors have equal eigenvalues. This electromagnetic symmetry includes that of hexagonal, tetragonal and trigonal crystals. These are said to be optically uniaxial.

5. Examples

[31] I consider $\sigma_1 = 0.2$ S/m, $\sigma_2 = 0.03$ S/m and $\sigma_3 = 0.05$ S/m, and $\mu = \mu_0 = 4\ \pi\ 10^{-7}$ H/m. The phase velocity, energy velocity and skin depth at the Cartesian planes are shown in Figure 1. The frequency is $f = 1$ Hz. The electric (magnetic) field is perpendicular to the plane for the TE (TM) mode (see Figure 1b). The first are isotropic while the TM modes show anisotropy. Both the velocity and skin depth decrease for increasing conductivity. This means, for instance, that the diffusion process is slower in salt water than in fresh water, or slower in brine-saturated sediments than in oil-saturated reservoirs. On the other hand, the velocity increases and the skin depth decreases with the frequency.

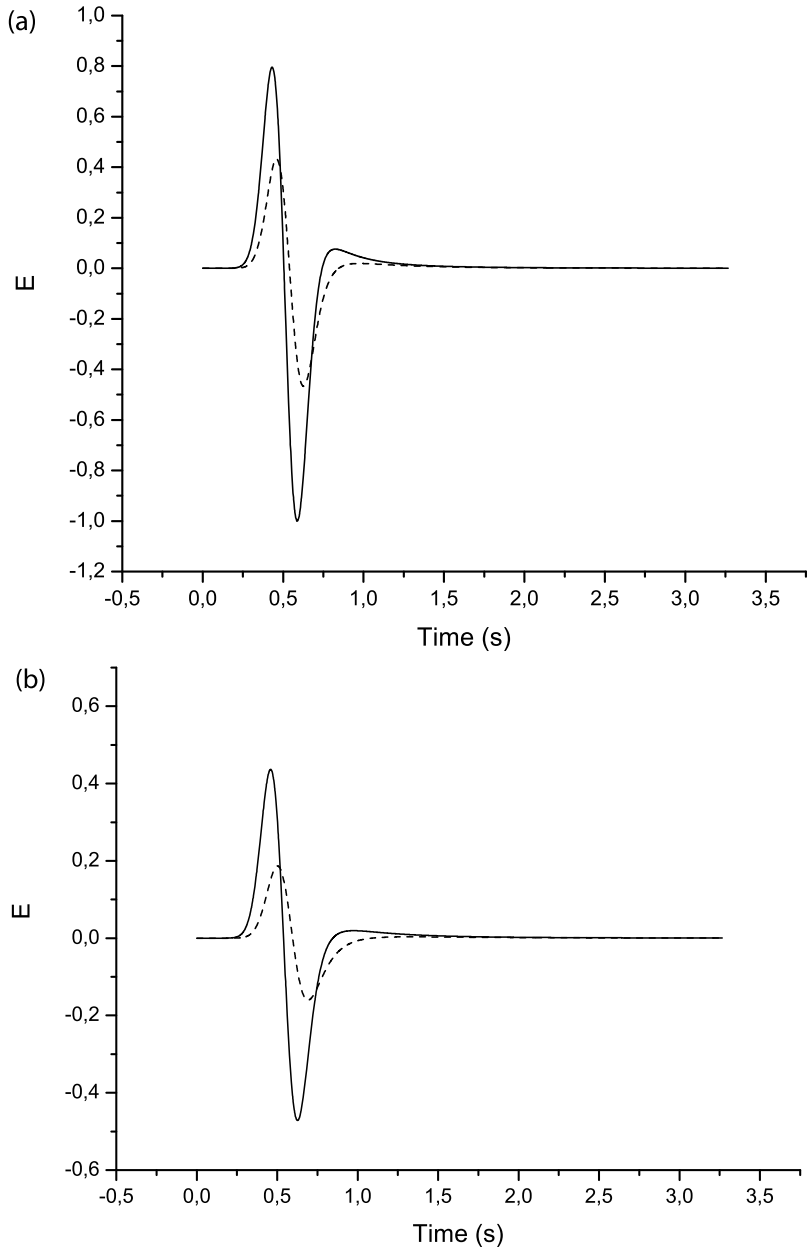

Figure 2. Electric field as a function of propagation time at (a) $(x, y, z) = (2, 1, 1)$ km and (b) $(x, y, z) = (3, 1, 1)$ km from the source location. The solid and dashed lines correspond to the anisotropic and isotropic cases, respectively.

[32] Let us consider a transient source, whose time history is

$$h(t) = \left(a - \frac{1}{2}\right)\exp(-a), \quad a = \left[\frac{\pi(t - t_s)}{t_p}\right]^2, \quad (66)$$

where t_p is the period of the wave (the distance between the side peaks is $\sqrt{6}t_p/\pi$) and I take $t_s = 1.4t_p$. I consider $\sigma_1 = \sigma_2 = 0.1$ S/m and $\sigma_3 = 0.05$ S/m and a central frequency $f_p = 3$ Hz. Figure 2 shows the time history at two different distances from the source location, corresponding to the anisotropic and isotropic cases (solid and dashed lines, respectively). The electric field is normal-

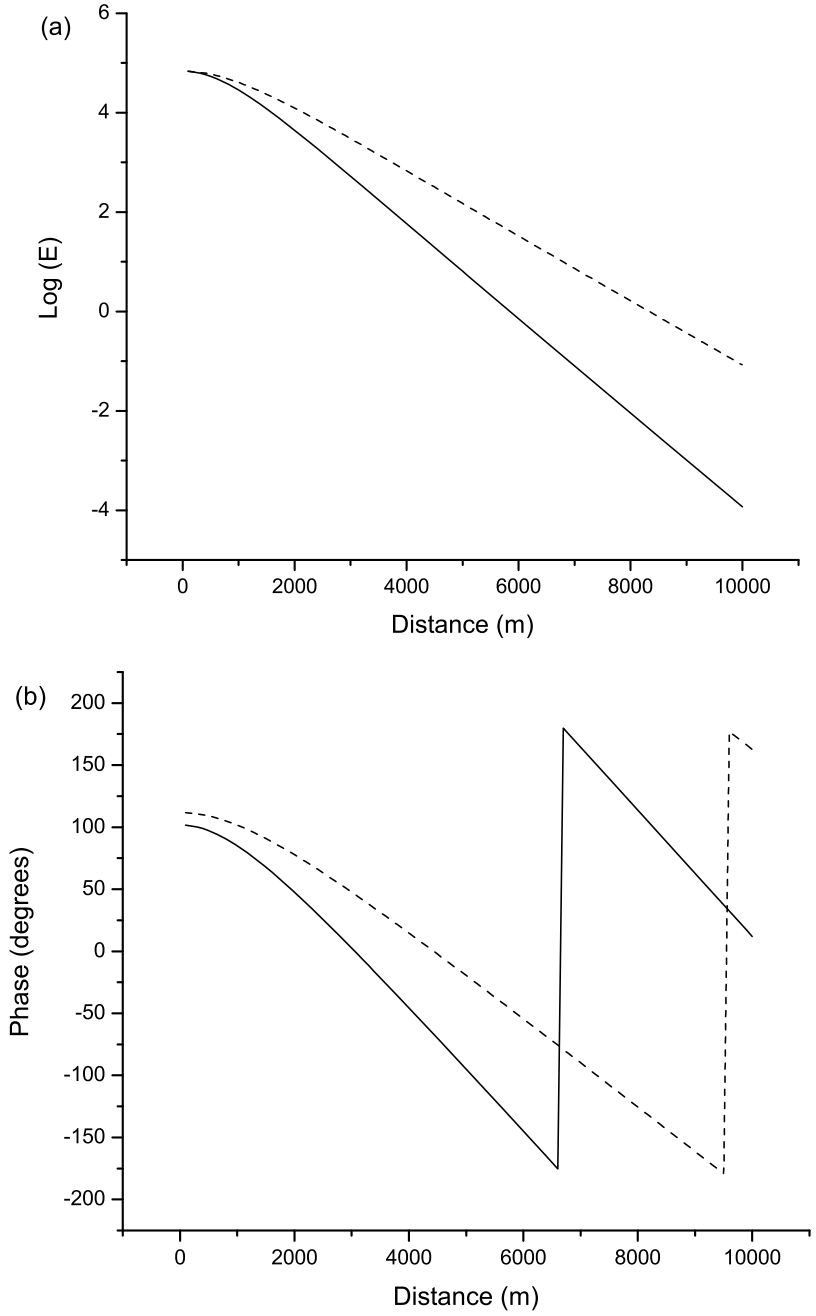

Figure 3. (a) AVO and (b) PVO responses along the x direction (solid lines) compared to the isotropic case (dashed lines). The frequency is 2 Hz and $(y, z) = (1, 1)$ km.

ized with respect to maximum amplitude. Isotropy corresponds to $\sigma_1 = \sigma_3 = 0.1$ S/m. The amplitude and phase variations with offset are shown in Figure 3. As can be appreciated, the differences can be substantial.

6. Conclusions

[33] The study of electromagnetic propagation in anisotropic media requires a detailed plane-wave analysis and the establishment of the energy balance to obtain the expression of measurable quantities such as the energy velocity as a function of frequency and propagation direction. In the case of uniform plane waves, the stored and dissipated energies have the same value. Fundamental relations are obtained, e.g., the energy density can be obtained as the scalar product of the slowness and the power-flow vectors. For uniform waves, one of the relations indicates that the energy velocity and slowness surfaces are reciprocal.

[34] The theory can be generalized to the case of induced polarization, i.e., a complex and frequency-dependent conductivity tensor. The generalization is straightforward. In this case, the stored electric energy is not zero and the magnetic stored energy does not have the same value of the dissipated energy. In terms of mechanical models, it can be shown that the conductivity components can be represented by Kelvin-Voigt elements.

[35] A closed form solution is obtained in the time domain for a uniaxial (transversely isotropic) medium. The solution is useful to obtain amplitude and phase variations as a function of the propagation distance (offset) in the frequency domain.

[36] The examples illustrate the differences between the anisotropic and isotropic cases, which can be significant.

Appendix A: Equivalence Between the Stored and Dissipated Energy Densities

[37] I show here that, for uniform plane waves and a real conductivity tensor, the stored energy equals the dissipated energy over a cycle. The magnetic energy (43) is

$$u_m = \frac{1}{4}\mu|\mathbf{H}|^2 = \frac{1}{4}\left[|\boldsymbol{\xi}|^2|\mathbf{E}|^2 - |\boldsymbol{\xi}\cdot\mathbf{E}^*|^2\right], \qquad \text{(A1)}$$

where I have used equation (17) and the property $(\mathbf{A}\times\mathbf{B})\cdot(\mathbf{C}\times\mathbf{D}) = (\mathbf{A}\cdot\mathbf{C})(\mathbf{B}\cdot\mathbf{D}) - (\mathbf{A}\cdot\mathbf{D})(\mathbf{B}\cdot\mathbf{C})$. On the other hand, the electric energy (46) is

$$u_e = \frac{1}{4}\mathbf{E}\cdot\frac{\boldsymbol{\sigma}}{\omega}\cdot\mathbf{E}^* = -\frac{\imath}{4}\left[(\boldsymbol{\xi}\cdot\mathbf{E})(\boldsymbol{\xi}\cdot\mathbf{E}^*) - (\boldsymbol{\xi}\cdot\boldsymbol{\xi})|\mathbf{E}|^2\right], \qquad \text{(A2)}$$

where I have used equation (20), the fact that $\boldsymbol{\sigma}$ is real and the property $\mathbf{A}\times(\mathbf{B}\times\mathbf{C}) = (\mathbf{A}\cdot\mathbf{C})\mathbf{B} - (\mathbf{A}\cdot\mathbf{B})\mathbf{C}$.

[38] From equations (31) and (32), it is $\boldsymbol{\xi} = (1-\imath)s\hat{\boldsymbol{\xi}}$ and $|\boldsymbol{\xi}|^2 = \imath\boldsymbol{\xi}\cdot\boldsymbol{\xi}$. Then, the last equation and $|\boldsymbol{\xi}\cdot\mathbf{E}^*|^2 = \imath(\boldsymbol{\xi}\cdot\mathbf{E})(\boldsymbol{\xi}\cdot\mathbf{E}^*)$ imply

$$u_m = u_e. \qquad \text{(A3)}$$

[39] **Acknowledgment.** This work was funded by EMGS ASA.

References

Abramovici, F. (1974), The forward magnetotelluric problem for an inhomogeneous and anisotropic structure, *Geophysics*, *39*, 56–68.

Anderson, B., T. Barber, and S. Gianzero (2001), The effect of crossbedding anisotropy on induction tool response, *Petrophysics*, *42*, 137–149.

Badea, E. A., M. E. Everett, G. A. Newman, and O. Biro (2001), Finite-element analysis of controlled-source electromagnetic induction using Coulomb-gauged potentials, *Geophysics*, *166*, 786–799.

Carcione, J. M. (1996), Ground penetrating radar: Wave theory and numerical simulation in conducting anisotropic media, *Geophysics*, *61*, 1664–1677.

Carcione, J. M. (2007), *Wave Fields in Real Media: Wave Propagation in Anisotropic, Anelastic, Porous, and Electromagnetic Media*, 2nd ed., Elsevier, Amsterdam.

Carcione, J. M., and F. Cavallini (1995), On the acoustic-electromagnetic analogy, *Wave Motion*, *21*, 149–162.

Carcione, J. M., and K. Helbig (2008), Elastic medium equivalent to Fresnels double-refraction crystal, *J. Acoust. Soc. Am.*, *124*(4), 2053–2060.

Carcione, J. M., and M. Schoenberg (2000), 3-D ground-penetrating radar simulation and plane wave theory, *Geophysics*, *65*, 1527–1541.

Carcione, J. M., and G. Seriani (2000), An electromagnetic modelling tool for the detection of hydrocarbons in the subsoil, *Geophys. Prospect.*, *48*, 231–256.

Carslaw, H. S., and J. C. Jaeger (1984), *Conduction of Heat in Solids*, Clarendom Press, Oxford, U. K.

Davydycheva, S., V. Druskin, and T. Habashy (2003), An efficient finite-difference scheme for electromagnetic logging in 3D anisotropic inhomogeneous media, *Geophysics*, *68*, 1525–1536.

Eidesmo, T., S. Ellingsrud, L. M. MacGregor, S. Constable, M. C. Sinha, S. Johansen, F. N. Kong, and H. Westerdahl (2002), Sea bed logging (SBL), a new method for remote and direct identification of hydrocarbon filled layers in deepwaters areas, *First Break*, *20*, 144–151.

Kováčiková, S., and J. Pek (2002), Generalized Riccati equations for 1-D magnetotelluric impedances over anisotropic conductors, part I: Plane wave field model, *Earth Planets Space*, *54*, 473–482.

Loewenthal, D., and M. Landisman (1973), Theory of magnetotelluric observations on the surface of a layered anisotropic half-space, *Geophys. J. R. Astron. Soc.*, *35*, 195–214.

Mackie, R. L., T. R. Madden, and P. E. Wannamaker (1993), Three-dimensional magnetotelluric modeling using finite difference equations: Theory and comparisons to integral equation solutions, *Geophysics*, *58*, 215–226.

Mann, J. E., Jr. (1965), The importance of anisotropic conductivity in magnetotelluric interpretation, *J. Geophys. Res.*, *15*, 2940–2942.

Negi, J. G., and P. D. Saraf (1989), *Anisotropy in Geoelectromagnetism*, Elsevier, New York.

Olhoeft, G. R., and D. E. Capron (1994), Petrophysical causes of electromagnetic dispersion, paper presented at Fifth International Conference on Ground Penetrating Radar, Univ. of Waterloo, Kitshener, Ont., Canada, 12–16 Jun.

Oristaglio, M. L., and G. W. Hohmann (1984), Diffusion of electromagnetic fields into a two-dimensional Earth: A finite-difference approach, *Geophysics*, *49*, 870–894.

Pellerin, L., J. M. Johnston, and G. W. Hohmann (1996), A numerical evaluation of electromagnetic methods in geothermal exploration, *Geophysics*, *61*, 121–130.

Stalnaker, J. L. (2004), A finite element approach to the 3D CSEM modeling problem and applications to the study of the effect of target interaction and topography, Ph.D. thesis, Texas A&M Univ., College Station, Tex.

Wang, T., and S. Fang (2001), 3D electromagnetic anisotropy modeling using finite differences, *Geophysics*, *66*, 1386–1398.

Wang, T., and J. Signorelli (2004), Finite-difference modeling of electromagnetic tool response for logging while drilling, *Geophysics*, *69*, 152–160.

Ward, S. H., and G. W. Hohmann (1988), Electromagnetic theory for geophysical applications, in *Electromagnetic Methods in Applied Geophysics*, edited by M. N. Nabighian, pp. 313–364, Soc. of Explor. Geophys., Tulsa, Okla.

Weidelt, P. (1998), Three-dimensional conductivity models: Implications of electrical anisotropy, in *3D Electromagnetics*, edited by M. Oristaglio and B. Spies, pp. 1–11, Soc. of Explor. Geophys., Tulsa, Okla.

Weiss, C. J., and G. A. Newman (2002), Electromagnetic induction in a fully 3D anisotropic Earth, *Geophysics*, *67*, 1104–1114.

Yin, C., and H. M. Maurer (2001), Electromagnetic induction in a layered Earth with arbitrary anisotropy, *Geophysics*, *66*, 1405–1416.

Zhdanov, M. (2008), Generalized effective-medium theory of induced polarization, *Geophysics*, *73*, F197–F211.

J. M. Carcione, Istituto Nazionale di Oceanografia e di Geofisica Sperimentale, Borgo Grotta Gigante 42/C, 34010 Sgonico, I-34016 Trieste, Italy. (jcarcione@inogs.it)